Fluorine and related complexes in α-Al_2O_3

Minseok Choi[1,2*] and Chris G. Van de Walle[2†]

[1] *Department of Physics, Inha University, Incheon 22212, Korea and*

[2] *Materials Department, University of California, Santa Barbara, CA 93106-5050, USA*

(Dated: July 24, 2023)

Abstract

Using first-principles calculations based on hybrid-density-functional theory, we examine the energetics and electronic structure of fluorine in α-Al_2O_3. The F atom can be incorporated as an interstitial (F_i) or substitutional impurity on the oxygen site (F_O); the latter tends to be lower in energy, particularly under Al-rich conditions. Fluorine on the oxygen site acts as a donor, but for Fermi level positions high in the band gap a negatively charged DX configuration is lower in energy. Fluorine substituting on the Al site is not energetically stable. We also examine complexes between F and hydrogen or carbon, which can easily be unintentionally incorporated during growth or processing. Our calculated defect levels, combined with band alignments, allow us to assess the impact on Al_2O_3/semiconductor heterostructures. We find that F can passivate oxygen-vacancy related traps in the Al_2O_3 dielectric. Complex formation with H or C is either ineffective or could even be detrimental.

ACCEPTED MANUSCRIPT

Journal of Applied Physics

AIP Publishing

This is the author's peer reviewed, accepted manuscript. However, the online version of record will be different from this version once it has been copyedited and typeset.

PLEASE CITE THIS ARTICLE AS DOI: 10.1063/5.0161929

ACCEPTED MANUSCRIPT
Journal of Applied Physics
AIP Publishing
This is the author's peer reviewed, accepted manuscript. However, the online version of record will be different from this version once it has been copyedited and typeset.
PLEASE CITE THIS ARTICLE AS DOI: 10.1063/5.0161929

I. INTRODUCTION

Understanding the behavior of defects and impurities in Al_2O_3 is crucial for many applications. Al_2O_3 and $(Al_xGa_{1-x})_2O_3$ alloys are used as carrier confinement layers in Ga_2O_2-based devices, which have attracted a lot of attention for high-power electronics.[1] Knowing the impact of defects and impurities on electronic properties is essential for controlling doping in these layers. Al_2O_3 is also used as the gate dielectric in GaN- and SiC-based metal-oxide-semiconductor field-effect transistors (MOSFETs).[2,3] The quality of the oxide dielectric and of its interface with the semiconductor channel is critical for device performance, since defects or impurities can act as carrier traps, cause current leakage, or scatter carriers..[4–9] It was shown that oxygen vacancies (V_O) act as charge traps and cause carrier leakage,[8] cation vacancies lead to fixed charge,[10] and impurities such as carbon result in border traps or leakage current.[9,11–14]

While a number of impurities have already been investigated in Al_2O_3, fluorine (F) has thus far received little attention. Our interest in F is twofold. First, it can be expected to act as an active dopant, particularly as a donor when incorporated on the oxygen site[15] or as an acceptor on interstitial sites.[16] Second, it may serve as a passivating agent, similar to the role played by hydrogen.[17–19] Experiments have shown that annealing in H_2 or forming gas after Al_2O_3 deposition improves the electrical properties of MOS devices.[20–24]Hydrogen can passivate defect states related to oxygen vacancies[13] or cation vacancies[25] in the oxide, dangling bonds at the interface,[26] and carbon-related carrier traps.[13,14,18]

Fluorine treatment has similarly been shown to improve the electrical properties of devices. In GaN-based high-electron-mobility transistors (HEMTs) with Al_2O_3 gate dielectrics, incorporation of F resulted in a high threshold voltage and better temperature stability.[27–29] Zhang *et al.* showed that the intrinsic positive charges in Al_2O_3 gate dielectric can be compensated by F ions in GaN MOS-HEMTs.[30] They proposed that negatively-charged F ions diffused into the oxide from the AlGaN barrier during the 250 °C atomic layer deposition (ALD) compensate the intrinsic positive charge present in the Al_2O_3. However, an understanding of the microscopic structure and the mechanisms by which F affects the properties of Al_2O_3 is still lacking.

In this work, we present a first-principles study based on hybrid-density-functional theory of F in Al_2O_3, as well as the interaction between F and native point defects (V_O and V_{Al}) and

ACCEPTED MANUSCRIPT
Journal of Applied Physics
AIP Publishing
This is the author's peer reviewed, accepted manuscript. However, the online version of record will be different from this version once it has been copyedited and typeset.
PLEASE CITE THIS ARTICLE AS DOI: 10.1063/5.0161929

with other impurities, leading to formation of F–H and F–C complexes. We examine formation energies and charge-state transition levels, and compare the results with experiments on GaN- and SiC- based MOS devices.

We focus on α-Al_2O_3, i.e., the corundum phase. In the context of Ga_2O_3-based devices, the monoclinic phase has been widely investigated because of the availability of high-quality substrates.[31,32] However, achieving a high Al content in β-$(Al_xGa_{1-x})_2O_3$ alloys has proven challenging.[33] In contrast, growth of corundum-phase α-$(Al_xGa_{1-x})_2O_3$ alloys on sapphire substrates has been demonstrated over the entire composition range.[34,35] Examining impurities in the corundum phase is thus highly relevant.

In the context of use of Al_2O_3 as a dielectric, the widely used ALD technique most likely results in amorphous films, while metal-organic chemical vapor deposition (MOCVD) yields polycrystalline material. While detailed structural characterization is lacking, it is reasonable to expect that Al_2O_3 will crystallize in its most stable phase, i.e., corundum. As for amorphous structures, we argue that since the local environment is similar to that in the crystalline material, results for impurities in the crystalline phase are relevant, and the most stable corundum phase is a reasonable choice.

II. COMPUTATIONAL APPROACH

First-principles density functional theory calculations were carried out using the screened hybrid functional of Heyd-Scuseria-Ernzerhof (HSE),[36,37] implemented with the projector augmented-wave method[38] in the VASP code.[39] The electronic wave functions were expanded in a plane-wave basis set with an energy cutoff of 400 eV. The HSE mixing parameter was set to 32%,[8] resulting in a band gap of 9.18 eV in α-Al_2O_3, which is close to the experimentally reported values of 8.8 eV.[40]

The conventional unit cell of α-Al_2O_3 contains 30 atoms. The calculated lattice parameters a = 4.74 Å and c = 12.94 Å agree with the experimental values of a = 4.76 Å and c = 12.99 Å.[41] Each Al is bonded to six O and each O is surrounded by four Al, and the calculated Al–O bond lengths are 1.85 Å for three shorter and 1.96 Å for three longer bonds around each Al atom, close to the experimental values of 1.86 and 1.97 Å.[41]

Impurity calculations were performed using periodic boundary conditions with supercells that contain 120 atoms. The supercells were constructed by first rotating the **a** lattice vector

AIP Publishing
Journal of Applied Physics
ACCEPTED MANUSCRIPT
This is the author's peer reviewed, accepted manuscript. However, the online version of record will be different from this version once it has been copyedited and typeset.
PLEASE CITE THIS ARTICLE AS DOI: 10.1063/5.0161929

of the conventional cell by 30° (to obtain a cell with orthogonal lattice vectors), and then taking a $\sqrt{3} \times 2 \times 1$ multiple of this cell. The integrations over the Brillouin zone were performed using a 2×2×1 k-point grid. Spin polarization was included.

The formation energy of a defect or impurity X in charge state q is given by:[42]

$$E^f(X^q) = E_{\rm tot}(X^q) - E_{\rm tot}({\rm Al_2O_3}) - \sum_i n_i(\mu_i^0 + \mu_i) + q\epsilon_F + \Delta^q, \quad (1)$$

where $E_{\rm tot}(X^q)$ is the total energy of a supercell containing the defect X in charge state q, and $E_{\rm tot}({\rm Al_2O_3})$ is the total energy of the pristine Al_2O_3 in the same supercell. n_i is the number of atoms of type i added (n_i>0) to or removed from (n_i<0) the pristine Al_2O_3, and μ_i is the atomic chemical potential. These atomic chemical potentials are referenced to the energy per atom μ_i^0 in the elemental phases, i.e., Al metal for Al and an isolated O_2 molecule for O. In principle the $\mu_{\rm Al}$ and $\mu_{\rm O}$ chemical potentials are variables, reflecting the relative abundance of the constituents during growth or processing. They must satisfy the stability condition of Al_2O_3, $2\mu_{\rm Al}+3\mu_{\rm O}=\Delta H_f({\rm Al_2O_3})$ with $\mu_{\rm Al}\leq 0$ and $\mu_{\rm O}\leq 0$. For purposes of presenting our results, we will show values for extreme O-rich (Al-poor) conditions [$\mu_{\rm O}=0$ and $\mu_{\rm Al}=(1/2)\Delta H_f({\rm Al_2O_3})$] and for extreme O-poor (Al-rich) conditions [$\mu_{\rm O}=(1/3)\Delta H_f({\rm Al_2O_3})$ and $\mu_{\rm Al}=0$]. The calculated formation enthalpy of α-Al_2O_3, $\Delta H_f({\rm Al_2O_3})=-16.22$ eV/f.u. is in good agreement with the experimental value of −17.04 eV.[43] To examine growth conditions corresponding to specific values of $\mu_{\rm Al}$ and $\mu_{\rm O}$, the formation energies can be readily obtained by referring back to Eq. (1).

Values for the impurity chemical potential were chosen based on equilibrium with AlF_3 for F, H_2 for H, and diamond for C.[9,18] ϵ_F is the Fermi level referenced to the valence-band maximum (VBM), and Δ^q is the correction term to align the electrostatic potentials of the pristine and defective supercells and to account for finite-cell size effects.[44,45]

The charge-state transition level (q/q') is defined as the Fermi-level position below which the defect is most stable in charge state q and above which the same defect is stable in charge state q':

$$(q/q') = \frac{E^f(X^q;\epsilon_F=0) - E^f(X^{q'};\epsilon_F=0)}{(q'-q)}, \quad (2)$$

where $E^f(X^q;\epsilon_F=0)$ is the formation energy for X^q when ϵ_F is at the VBM. The charge-state transition levels are not affected by the choice of chemical potentials.

ACCEPTED MANUSCRIPT
Journal of Applied Physics
AIP Publishing
This is the author's peer reviewed, accepted manuscript. However, the online version of record will be different from this version once it has been copyedited and typeset.
PLEASE CITE THIS ARTICLE AS DOI: 10.1063/5.0161929

III. RESULTS AND DISCUSSION

A. Isolated Fluorine

For isolated F, we investigate both interstitial and substitutional configurations (Fig. 1). Interstitial F (in the negative charge state F_i^-) prefers to sit centrally between two Al atoms, with F–Al distances of 1.79 Å [Fig. 1(b)]. Fluorine substituting on the O site in the positive charge state (F_O^+) leads to outward relaxation of the surrounding four Al atoms [see Fig. 1(c)], with F–Al distances of 1.93 Å for Al_1 and Al_2, 2.17 Å for Al_3, and 2.16 Å for Al_4; these bond lengths are 4–10 % larger than the O–Al bond lengths in pristine Al_2O_3. In the − charge state (corresponding to the formation of a DX center),[46] F significantly distorts the atomic structure by breaking several F–Al and Al–O bonds [Fig. 1(d)]. The F–Al distances are 1.90 Å for Al_1 and 1.72 Å for Al_2, 2.88 Å for Al_3, and 2.44 Å for Al_4. The Al–O distances are 2.32 Å for O_1 and 2.39 Å for O_2.

Fluorine substituting on the Al site (F_{Al}) is found to be unstable. When placed on the substitutional Al site, the F atom spontaneously moves off-center. Based on formation energies we will see below that this configuration is not energetically stable.

Figure 2 shows the calculated formation energies for isolated F in α-Al_2O_3 as a function of the Fermi level, ranging from zero at the VBM to the value of the band gap at the conduction-band minimum (CBM). The formation energies of V_O and V_{Al} are added for comparison.[8] At each Fermi-level value we show only the formation energy of the charge state with lowest energy. The kinks in the curves correspond to the charge-state transition levels (Fig. 3), i.e., the defect levels of the impurity or defect in the band gap.

For F_i, the (+/0) and (0/−) levels occur at 1.67 eV and 2.29 eV above the VBM, indicating that F_i acts as an acceptor (F_i^-) for most Fermi-level positions in the band gap. F_O has a (+/−) level at 1.24 eV below the CBM, indicating that F_O acts as a donor (F_O^+) for most Fermi-level positions. The stability of the negative charge state at high Fermi-level positions is indicative of a DX state, in which an impurity expected to act as a shallow donor exhibits a large lattice relaxation and becomes negatively charged by trapping electrons, thus effectively acting as a deep acceptor.[46] As is common for a DX center, the neutral charge state of F_O is never thermodynamically stable, indicative of a "negative-U" center.

These results indicate that F_O will not act as a shallow donor in α-Al_2O_3—which would

ACCEPTED MANUSCRIPT
Journal of Applied Physics
AIP Publishing
This is the author's peer reviewed, accepted manuscript. However, the online version of record will be different from this version once it has been copyedited and typeset.
PLEASE CITE THIS ARTICLE AS DOI: 10.1063/5.0161929

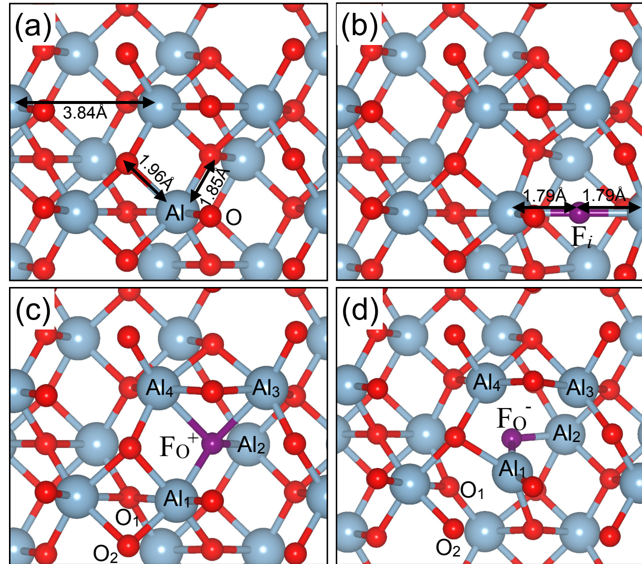

FIG. 1: Local atomic structure[47] for various configurations of F in α-Al_2O_3. (a) Pristine α-Al_2O_3; (b) F interstitial in the –1 charge state (F_i^-);(c) F on the O site in the +1 charge state (F_O^+); and (d) F on the O site in the –1 charge state (F_O^-).

be unlikely, because it is really an insulator with a very wide band gap. However, the high position of the (+/–) level indicates that when F_O is introduced in α-Al_2O_3 near a heterojunction with Ga_2O_3, F_O will act as a donor and the electron will go into the conduction band of Ga_2O_3 (modulation doping) (see Fig. 3). We note that under O-rich conditions the formation energy of F_O is very high, and there would also be a high risk of self-compensation by F_i. Therefore, if the goal is to intentionally incorporate F_O during growth, more Al-rich conditions should be used.

In order to examine the impact of F on devices, in Fig. 3 we plot the charge-state transition levels within the band gap of α-Al_2O_3 corresponding to the defects shown in Fig. 2. To assess which defects will be most relevant to devices, we align the bands of α-Al_2O_3 with the band edges of GaN, SiC, α-Ga_2O_3, and β-Ga_2O_3; the alignment was performed based on values in the literature.[8,48,49] Defects with levels that lie within the band gaps of the semiconductors would be most detrimental to devices. The Al vacancy (not shown in Fig. 3) has defect levels that are relatively low in the gap and would primarily act as a fixed-charge center.[8]

Figure 3 shows that V_O is of highest concern since it introduces states that can trap carriers. Fluorine treatment of Al_2O_3 may passivate these V_O-related carrier traps. Indeed,

ACCEPTED MANUSCRIPT
Journal of Applied Physics
AIP Publishing
This is the author's peer reviewed, accepted manuscript. However, the online version of record will be different from this version once it has been copyedited and typeset.
PLEASE CITE THIS ARTICLE AS DOI: 10.1063/5.0161929

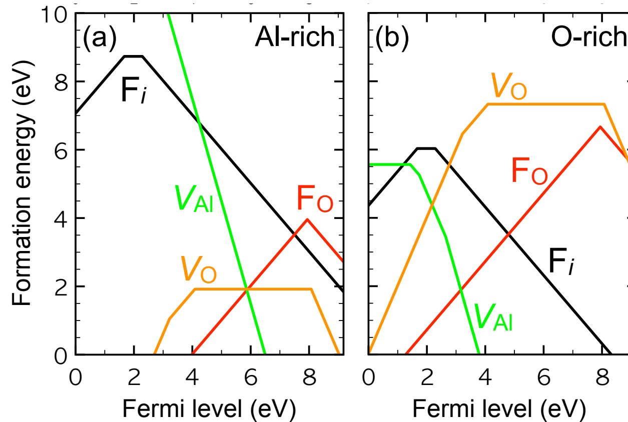

FIG. 2: Formation energies of fluorine in α-Al_2O_3 as a function of the Fermi-level position under (a) Al-rich and (b) O-rich condition. For comparison, the formation energies of native vacancies (V_{Al} and V_O) are added.[8]

when F is introduced in a post-growth treatment, it would diffuse as F_i and be attracted to any oxygen vacancies, which are then converted to F_O. Since F_O does not have defect levels in the range of the semiconductor band gaps, this amounts to passivation.

This mechanism may explain the experimentally observed improvements in device characteristics upon F treatment of GaN-based devices. Wang *et al.*[27] reported that in GaN-based HEMTs, F incorporation into Al_2O_3 led to a positive shift of the threshold voltage without current degradation. Another paper by the same group[28] demonstrated that for normally-off AlGaN/GaN HEMTs, F incorporation in the Al_2O_3 gate dielectric after argon plasma pre-treatment enabled achieving a high threshold voltage temperature stability. Wu *et al.*,[29] finally, suggested that light doping with F ions, which will incorporate as negatively charged interstitials (Fig. 2) would result in a high positive threshold voltage while preserving low ON-resistance.

B. F complexes with hydrogen

We also examined how fluorine interacts with hydrogen, which is commonly unintentionally present in layers that are grown with ALD or MOCVD; hydrogen may also be introduced during post-growth treatments such as forming-gas annealing. Figure 4(a) shows the local atomic structure of a neutral H–F_O complex, in which the H–F distance is 1.77 Å. The F–Al

ACCEPTED MANUSCRIPT
Journal of Applied Physics
AIP Publishing
This is the author's peer reviewed, accepted manuscript. However, the online version of record will be different from this version once it has been copyedited and typeset.
PLEASE CITE THIS ARTICLE AS DOI: 10.1063/5.0161929

distances are 2.03 Å for Al_1, 1.86 Å for Al_2, 1.92 Å for Al_3, and 2.82 Å for Al_4, indicating a significant distortion from the F_O^+ geometry. Notably, F broke the bond with the Al_4 atom, and got closer to another Al atom (Al*) with a distance of 2.60 Å. The H–Al distances are 1.56 Å to Al_4 and 1.76 Å to Al_1.

The atomic structure in the +2 charge state is quite different from that in the neutral charge state. The F atom bonds to four Al atoms, similar to the F_O^+ configuration, and H bonds to an O neighbor of Al_4 with a bond length of 0.99 Å. The resulting configuration is more like two separated F_O^+ and H_i^+ with a distance between H and F of 2.13 Å [Figs. 4(b) and (c)].

Figure 5 shows the calculated formation energy of the H–F_O complex as a function of the Fermi level in the band gap. The neutral H–F_O complex is stable for Fermi-level positions above 5.32 eV. The binding energy of this complex, using $E_{\rm bind}[(\mathrm{H}-\mathrm{F_O})^0] = E^f(\mathrm{H}_i^-) + E^f(\mathrm{F_O}^+) - E^f[(\mathrm{H}-\mathrm{F_O})^0]$, is 0.84 eV. The positive binding energy indicates that the interaction between H_i^- and ${F_O}^+$ is attractive and complex formation is energetically advantageous. Formation of the H–F_O complex would render the F_O donor electrically inactive. However, these complexes are not very likely to form after growth since H_i will

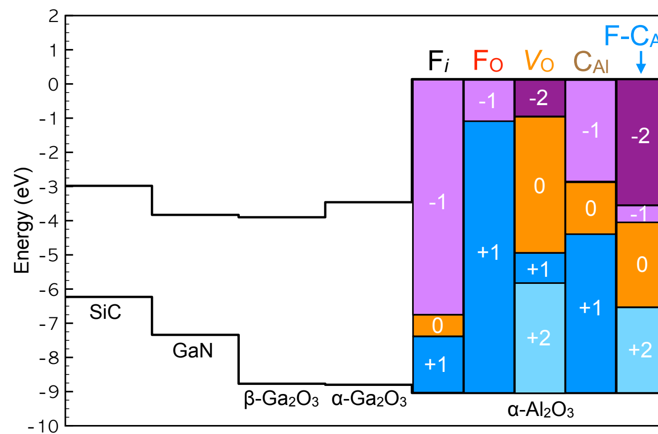

FIG. 3: Band alignment between semiconductors and α-Al_2O_3. For each material, the lower line corresponds to the VBM, the upper line to the CBM. Stable charge states and the position of charge-state transition levels for F and their complexes with H and C are shown within the oxide band gap.The positions of Ga compounds (GaN, α-Ga_2O_3, β-Ga_2O_3) and 4H-SiC band gap are shown with respect to the α-Al_2O_3 band edge, taken from Refs. 8, 48, and 49. The zero was set at the vacuum level.

ACCEPTED MANUSCRIPT
Journal of Applied Physics
AIP Publishing
This is the author's peer reviewed, accepted manuscript. However, the online version of record will be different from this version once it has been copyedited and typeset.
PLEASE CITE THIS ARTICLE AS DOI: 10.1063/5.0161929

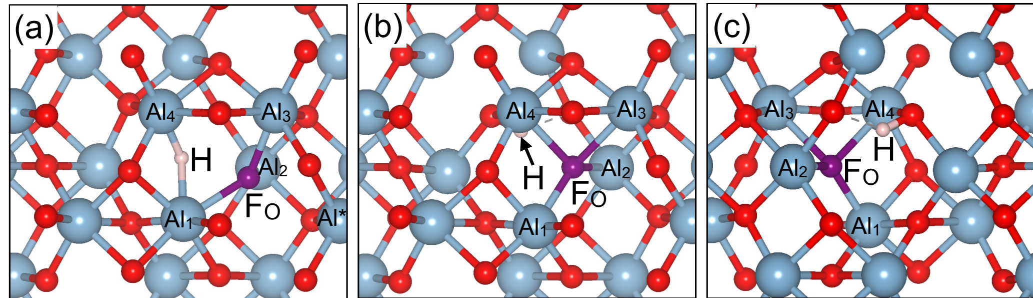

FIG. 4: Local atomic structures[47] of the H–F_O complex in α-Al_2O_3 in (a) the neutral, and (b) (c) the +2 charge state. (c) is the reverse view of (b).

predominantly occur in the positive charge state which is repelled by ${F_O}^+$.

With regard to the +2 charge state, the calculated binding energy in this case is negative ($E_{\rm bind}[(\rm H-F_O)^{+2}]$ = –0.30 eV), indicating that the sum of the formation energy of the constituents, ${F_O}^+$ and H_i^+, is smaller than the formation energy of the $(\rm H-F_O)^{+2}$ complex. We show the +2 charge state of this complex with dashed lines in Fig. 5, to emphasize that this is a locally stable configuration that is, however, thermodynamically unstable.

Finally, we comment on formation of (F_i–H_i) complexes. Since F_i is likely to occur in the negative charge state, and H_i in the positive charge state, such a complex is likely to form and be stable. The calculated binding energy for $(F_i\text{–}H_i)^0$ relative to F_i^- and H_i^+ is 0.22 eV.

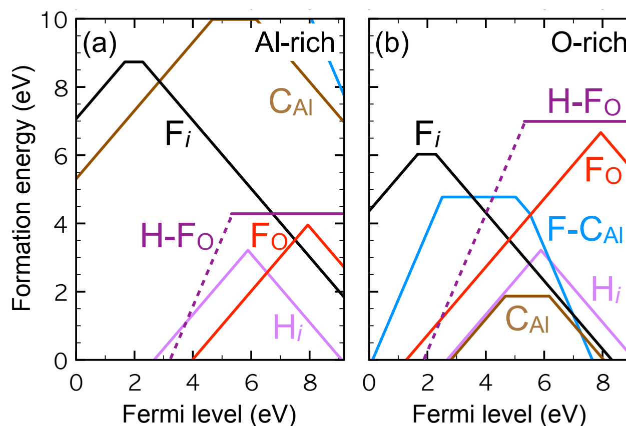

FIG. 5: Formation energies of F and its complexes with H and C in α-Al_2O_3 as a function of the Fermi-level position under (a) Al-rich and (b) O-rich condition. For comparison, the formation energies of a substitutional carbon impurity (C_{Al}) and interstitial H (H_i) are added.[8,9]

ACCEPTED MANUSCRIPT

Journal of Applied Physics

AIP Publishing

This is the author's peer reviewed, accepted manuscript. However, the online version of record will be different from this version once it has been copyedited and typeset.
PLEASE CITE THIS ARTICLE AS DOI: 10.1063/5.0161929

C. F complexes with Carbon

In a previous study we examined incorporation of carbon in α-Al_2O_3.[9] For purposes of our investigation of the effect of F treatments, we focus on C_{Al}, which is the most likely configuration for unintentionally incorporated C impurities in ALD-deposited Al_2O_3. In a typical ALD environment with O_2 gas at 270 °C at 1 Torr the chemical potential of oxygen would be μ_O = –0.65 eV,[8,9] which is relatively close to O-rich conditions.

For a complex between F and C_{Al} in the neutral charge state, we find that F bonds to C_{Al} with a bond length of 1.04 Å and C bonds to three O atoms with bond lengths of 1.40 Å [Fig. 6(a)]. The structure is quite similar to the H–C_{Al} complex reported in Ref.18 (in which the H–C and C–O bond lengths are 1.04 Å and 1.44 Å, respectively). In the negative charge state, the F–C_{Al} bond length is 1.27 Å, and the C–O_1 bond is broken with a distance of 2.42 Å; the remaining C–O bonds still have a bond length of $\sim$ 1.40 Å [Fig. 6(b)].

Results for formation energies of the F–C_{Al} complex are shown in Fig. 5. Three charge-state transition levels, (+2/0), (0/–), and (–/–2), are found at 2.51 eV, 5.02 eV, and 5.51 eV above the VBM, respectively. The calculated formation energy of the complex is quite high, but again this may not be relevant for the non-equilibrium conditions under which F is introduced in a post-growth treatment. What is more relevant is the binding energy between F and C. The binding energy can be calculated as $E_{\mathrm{bind}}[(\mathrm{F}-\mathrm{C_{Al}})^0] = E^f(\mathrm{F}_i^-) + E^f(\mathrm{C_{Al}}^+) - E^f[(\mathrm{F}-\mathrm{C_{Al}})^0]$, resulting in 0.74 eV. We assume here that interstitial F is introduced as a F_i^- ion. The positive binding energy indicates that the interaction between F_i^- and $C_{Al}{}^+$ is attractive and complex formation becomes energetically advantageous. The formation

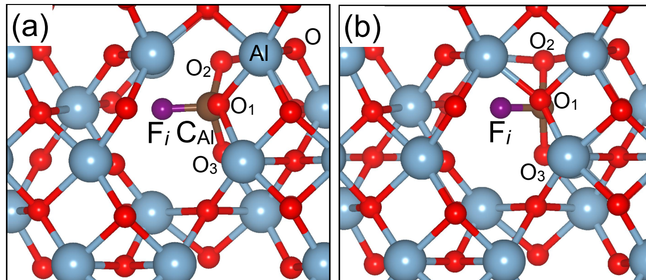

FIG. 6: Local atomic structures[47] of the F–C_{Al} complex in α-Al_2O_3 in (a) the neutral and (b) the –1 charge state.

ACCEPTED MANUSCRIPT
Journal of Applied Physics
AIP Publishing
This is the author's peer reviewed, accepted manuscript. However, the online version of record will be different from this version once it has been copyedited and typeset.
PLEASE CITE THIS ARTICLE AS DOI: 10.1063/5.0161929

of F–C_{Al} complexes may explain X-ray photoelectron spectroscopy measurements showing evidence of F–C peaks in ALD-deposited Al_2O_3 films after NF_3 plasma treatment.[50]

Figure 3 shows that the higher two levels of the F–C_{Al} complex are located in between the C_{Al} transition levels, near the CBM of the semiconductors. The (0/−) of the complex is at 0.30 eV below and the (−/−2) level at 0.19 eV above the GaN CBM; relative to the 4H-SiC CBM, (0/−) is at 1.04 eV and (−/−2) at 0.55 eV below the 4H-SiC CBM. This indicates that these levels can act as carrier traps in ALD-Al_2O_3-based MOS devices. Unlike hydrogen,[18] fluorine thus does not passivate carbon-induced traps in MOS devices.

IV. CONCLUSION

In summary, we performed hybrid functional calculations for fluorine and its complexes with H and C impurities in α-Al_2O_3 and discussed their impact on devices. Fluorine favors substituting on the O site, particularly under Al-rich conditions. Substitutional fluorine acts as a (deep) donor and could provide carriers to Ga_2O_3 through modulation doping. When F is introduced into Al_2O_3 dielectrics, it passivates oxygen vacancies, thus eliminating V_O-related carrier traps. We also investigated complexes with H and C, impurities that are commonly unintentionally incorporated during oxide deposition, annealing, or surface treatment. We find that F is not effective in eliminating carbon-induced states in the Al_2O_3 band gap, whose position near the conduction-band edge of relevant semiconductors can be detrimental to MOS devices.

Acknowledgments

This work was supported by Inha University Research Grant (INHA-68917) and by the GAME MURI of the Air Force Office of Scientific Research (FA9550-18-1-0479). This work used Stampede2 at TACC through allocation DMR070069 from the Advanced Cyberinfrastructure Coordination Ecosystem: Services & Support (ACCESS) program, which is supported by NSF grants 2138259, 2138286, 2138307, 2137603, and 2138296. We also acknowledge the use of the Center for Scientific Computing, supported by the California NanoSystems Institute, the NSF Materials Research Science and Engineering Centers (No. DMR1720256) at UC Santa Barbara, and the NSF under No. CNS1725797 and the KISTI

supercomputing center (grant no. KSC-2021-CRE-0458).

ACCEPTED MANUSCRIPT
Journal of Applied Physics
AIP Publishing
This is the author's peer reviewed, accepted manuscript. However, the online version of record will be different from this version once it has been copyedited and typeset.
PLEASE CITE THIS ARTICLE AS DOI: 10.1063/5.0161929

---

* Electronic address: minseok.choi@inha.ac.kr

† Electronic address: vandewalle@mrl.ucsb.edu

[1] Y. Zhang, C. Joishi, Z. Xia, M. Brenner, S. Lodha, and S. Rajan, Applied Physics Letters **112**, 233503 (2018).

[2] F. Roccaforte, P. Fiorenza, G. Greco, M. Vivona, R. Lo Nigro, F. Giannazzo, A. Patti, and M. Saggio, Applied Surface Science **301**, 9 (2014).

[3] D. kun Shi, Y. Wang, X. Wu, Z. yang Yang, X. ji Li, J. qun Yang, and F. Cao, Solid-State Electronics **180**, 107992 (2021).

[4] S. Oktyabrsky and D. Y. Peide, *Fundamentals of III-V semiconductor MOSFETs* (Springer, 2010).

[5] J. Robertson, *New High-K Materials for CMOS Applications* (Elsevier, 2011), pp. 132–176.

[6] C. G. Van de Walle, M. Choi, J. Weber, J. Lyons, and A. Janotti, Microelectron. Eng. **109**, 211 (2013).

[7] E. Caruso, J. Lin, S. Monaghan, K. Cherkaoui, F. Gity, P. Palestri, D. Esseni, L. Selmi, and P. K. Hurley, IEEE Transactions on Electron Devices **67**, 4372 (2020).

[8] M. Choi, A. Janotti, and C. G. Van de Walle, J. Appl. Phys. **113**, 044501 (2013).

[9] M. Choi, J. L. Lyons, A. Janotti, and C. G. Van de Walle, Appl. Phys. Lett. **102**, 142902 (2013).

[10] M. Choi, J. L. Lyons, A. Janotti, and C. G. Van de Walle, physica status solidi (b) **250**, 787 (2013).

[11] X. Liu, R. Yeluri, J. Kim, S. Lal, A. Raman, C. Lund, S. Wienecke, J. Lu, M. Laurent, S. Keller, et al., Applied Physics Letters **103**, 053509 (2013).

[12] X. Liu, J. Kim, R. Yeluri, S. Lal, H. Li, J. Lu, S. Keller, B. Mazumder, J. S. Speck, and U. K. Mishra, Journal of Applied Physics **114**, 164507 (2013).

[13] M. Uenuma, K. Takahashi, S. Sonehara, Y. Tominaga, Y. Fujimoto, Y. Ishikawa, and Y. Uraoka, AIP Advances **8**, 105103 (2018).

[14] T. Shibata, M. Uenuma, T. Yamada, K. Yoshitsugu, M. Higashi, K. Nishimura, and Y. Uraoka, Japanese Journal of Applied Physics **61**, 065502 (2022).

[15] Y. Kang and C. G. Van de Walle, Applied Physics Letters **111**, 152107 (2017).

AIP Publishing
Journal of Applied Physics
ACCEPTED MANUSCRIPT
This is the author's peer reviewed, accepted manuscript. However, the online version of record will be different from this version once it has been copyedited and typeset.
PLEASE CITE THIS ARTICLE AS DOI: 10.1063/5.0161929

[16] A. Janotti, E. Snow, and C. G. Van de Walle, Applied Physics Letters **95**, 172109 (2009).

[17] C. G. Van de Walle and J. Neugebauer, Annual Review of Materials Research **36**, 179 (2006).

[18] M. Choi, A. Janotti, and C. G. Van de Walle, ACS Applied Materials & Interfaces **6**, 4149 (2014).

[19] M. Choi, Current Applied Physics **39**, 154 (2022).

[20] T.-H. Hung, S. Krishnamoorthy, M. Esposto, D. Neelim Nath, P. Sung Park, and S. Rajan, Applied Physics Letters **102**, 072105 (2013).

[21] K.-K. Choi, J. Kee, C.-G. Park, and D. kee Kim, Applied Physics Express **8**, 045801 (2015).

[22] S. C. Heo, D. Lim, W. S. Jung, R. Choi, H.-Y. Yu, and C. Choi, Microelectronic Engineering **147**, 239 (2015).

[23] H. Yoshioka, M. Yamazaki, and S. Harada, AIP Advances **6**, 105206 (2016).

[24] M. I. Idris and A. Horsfall, Crystals **12**, 1111 (2022).

[25] A. Venzie, A. Portoff, M. Stavola, W. B. Fowler, J. Kim, D.-W. Jeon, J.-H. Park, and S. J. Pearton, Applied Physics Letters **120**, 192101 (2022).

[26] B. Shin, J. R. Weber, R. D. Long, P. K. Hurley, C. G. V. de Walle, and P. C. McIntyre, Appl. Phys. Lett. **96**, 152908 (2010).

[27] Y.-H. Wang, Y. C. Liang, G. S. Samudra, H. Huang, B.-J. Huang, S.-H. Huang, T.-F. Chang, C.-F. Huang, W.-H. Kuo, and G.-Q. Lo, IEEE Electron Device Letters **36**, 381 (2015).

[28] Y.-H. Wang, Y. C. Liang, G. S. Samudra, C.-F. Huang, W.-H. Kuo, and G.-Q. Lo, Applied Physics Letters **108**, 233507 (2016).

[29] C.-H. Wu, P.-C. Han, Q. H. Luc, C.-Y. Hsu, T.-E. Hsieh, H.-C. Wang, Y.-K. Lin, P.-C. Chang, Y.-C. Lin, and E. Y. Chang, IEEE Journal of the Electron Devices Society **6**, 893 (2018).

[30] Y. Zhang, M. Sun, S. J. Joglekar, T. Fujishima, and T. Palacios, Applied Physics Letters **103**, 033524 (2013).

[31] Z. Galazka, R. Uecker, D. Klimm, K. Irmscher, M. Naumann, M. Pietsch, A. Kwasniewski, R. Bertram, S. Ganschow, and M. Bickermann, ECS Journal of Solid State Science and Technology **6**, Q3007 (2016).

[32] S. Mu, M. Wang, J. B. Varley, J. L. Lyons, D. Wickramaratne, and C. G. Van de Walle, Phys. Rev. B **105**, 155201 (2022).

[33] A. F. M. A. U. Bhuiyan, Z. Feng, J. M. Johnson, H.-L. Huang, J. Sarker, M. Zhu, M. R. Karim, B. Mazumder, J. Hwang, and H. Zhao, APL Materials **8**, 031104 (2020).

AIP Publishing
Journal of Applied Physics
ACCEPTED MANUSCRIPT
This is the author's peer reviewed, accepted manuscript. However, the online version of record will be different from this version once it has been copyedited and typeset.
PLEASE CITE THIS ARTICLE AS DOI: 10.1063/5.0161929

[34] R. Jinno, C. S. Chang, T. Onuma, Y. Cho, S.-T. Ho, D. Rowe, M. C. Cao, K. Lee, V. Protasenko, D. G. Schlom, et al., Science Advances **7**, eabd5891 (2021).

[35] A. F. M. A. U. Bhuiyan, Z. Feng, H.-L. Huang, L. Meng, J. Hwang, and H. Zhao, APL Materials **9**, 101109 (2021).

[36] J. Heyd, G. E. Scuseria, and M. Ernzerhof, J. Chem. Phys. **118**, 8207 (2003).

[37] A. V. Krukau, O. A. Vydrov, A. F. Izmaylov, and G. E. Scuseria, J. Chem. Phys. **125**, 224106 (2006).

[38] P. E. Blöchl, Phys. Rev. B **50**, 17953 (1994).

[39] G. Kresse and J. Hafner, Phys. Rev. B **48**, 13115 (1993).

[40] R. H. French, J. Am. Ceram. Soc. **73**, 477 (1990).

[41] R. E. Newnham and Y. M. de Haan, Z. Kristallogr. **117**, 235 (1962).

[42] C. Freysoldt, B. Grabowski, T. Hickel, J. Neugebauer, G. Kresse, A. Janotti, and C. G. Van de Walle, Rev. Mod. Phys. **86**, 253 (2014).

[43] D. Ghosh and D. A. R. Kay, J. Electrochem. Soc. **124**, 1836 (1977).

[44] C. Freysoldt, J. Neugebauer, and C. G. Van de Walle, Phys. Rev. Lett. **102**, 016402 (2009).

[45] C. Freysoldt, J. Neugebauer, and C. G. Van de Walle, phys. status solidi (b) **248**, 1067 (2011).

[46] D. J. Chadi and K. J. Chang, Phys. Rev. Lett. **61**, 873 (1988).

[47] K. Momma and F. Izumi, J. Appl. Cryst. **44**, 1272 (2011).

[48] E. Kojima, K. Endo, H. Shirakawa, K. Chokawa, M. Araidai, Y. Ebihara, T. Kanemura, S. Onda, and K. Shiraishi, Journal of Crystal Growth **468**, 758 (2017).

[49] H. Peelaers, J. B. Varley, J. S. Speck, and C. G. Van de Walle, Applied Physics Letters **112**, 242101 (2018).

[50] J. Kim, D. Shim, Y. Kim, and H. Chae, Journal of Vacuum Science & Technology A **40**, 032603 (2022).

ACCEPTED MANUSCRIPT
Journal of Applied Physics
AIP Publishing
This is the author's peer reviewed, accepted manuscript. However, the online version of record will be different from this version once it has been copyedited and typeset.
PLEASE CITE THIS ARTICLE AS DOI: 10.1063/5.0161929

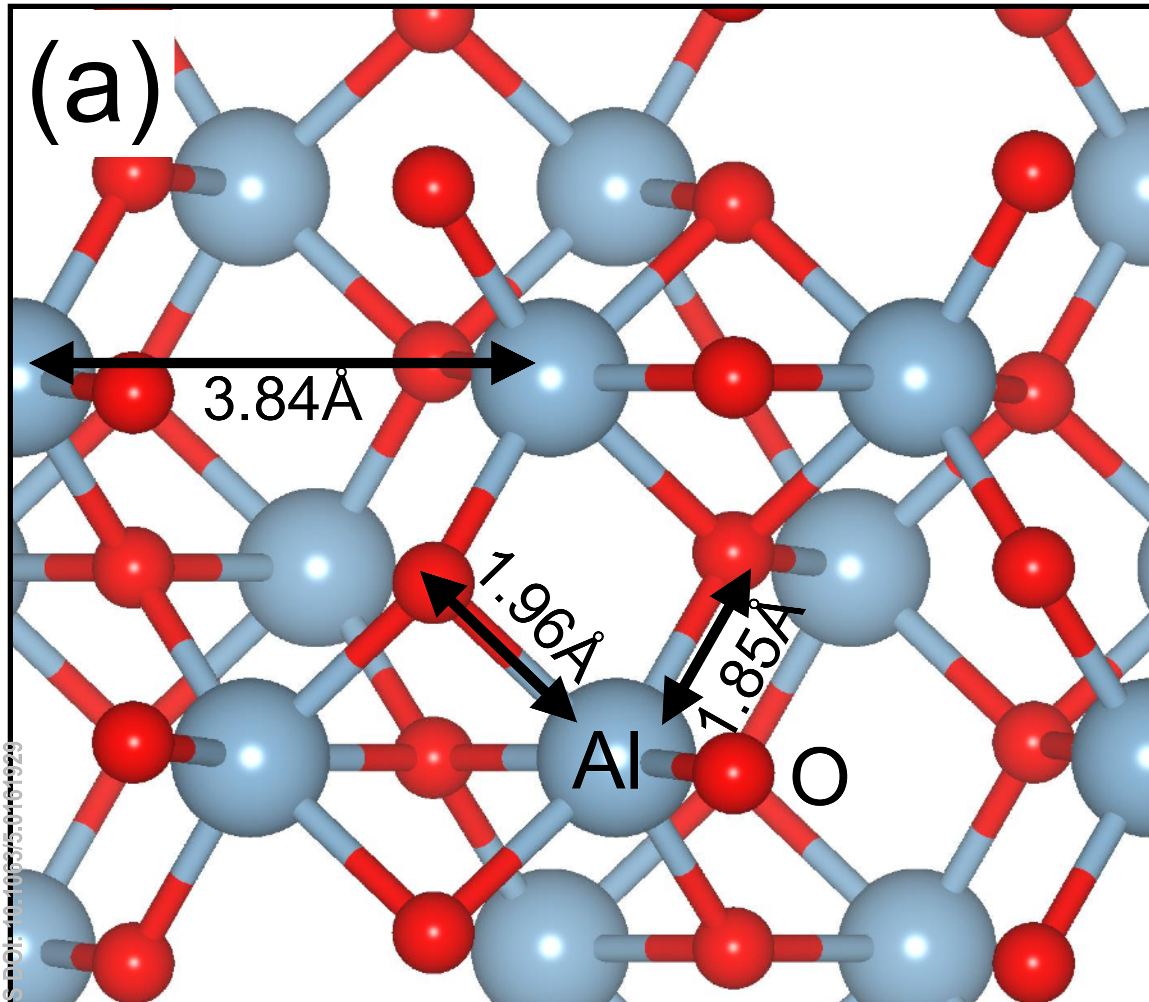

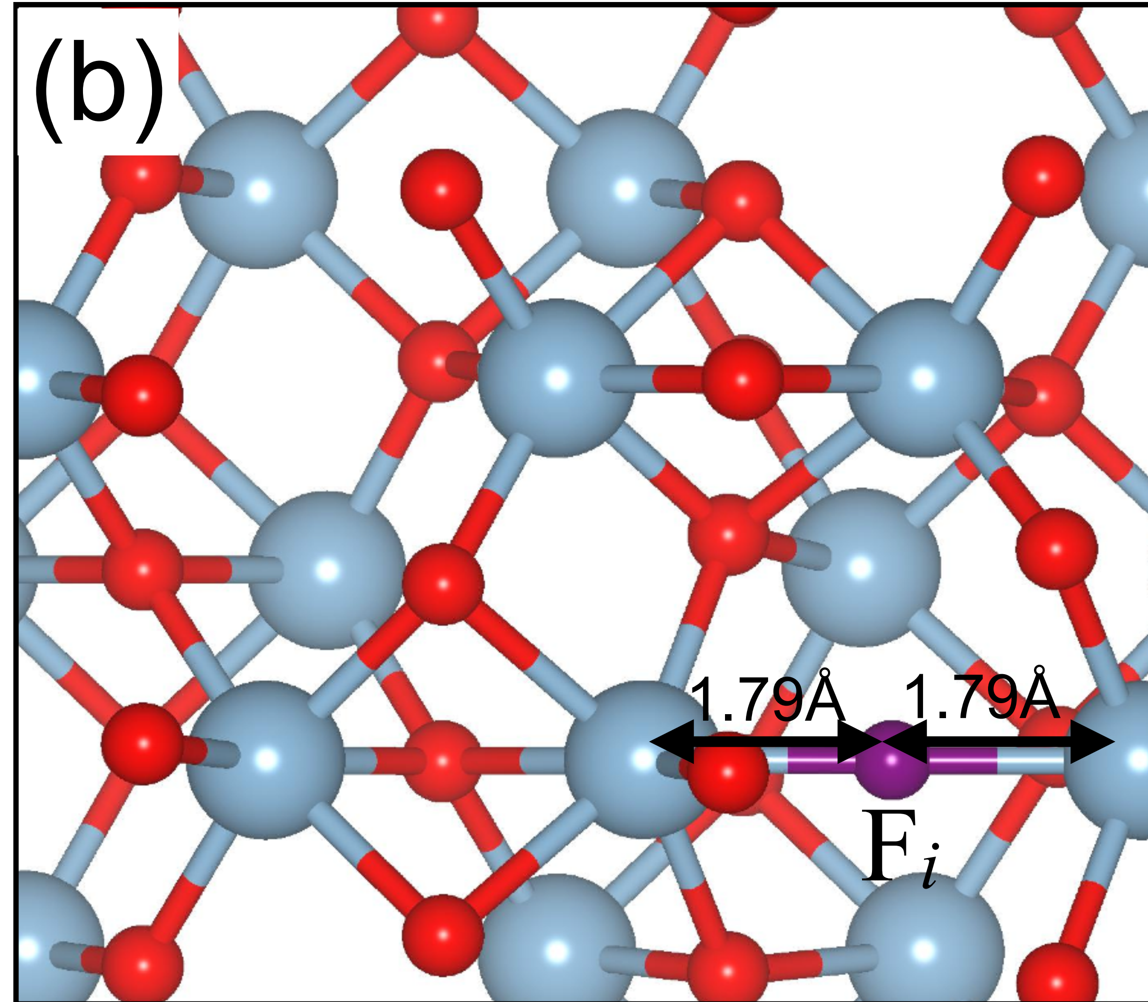

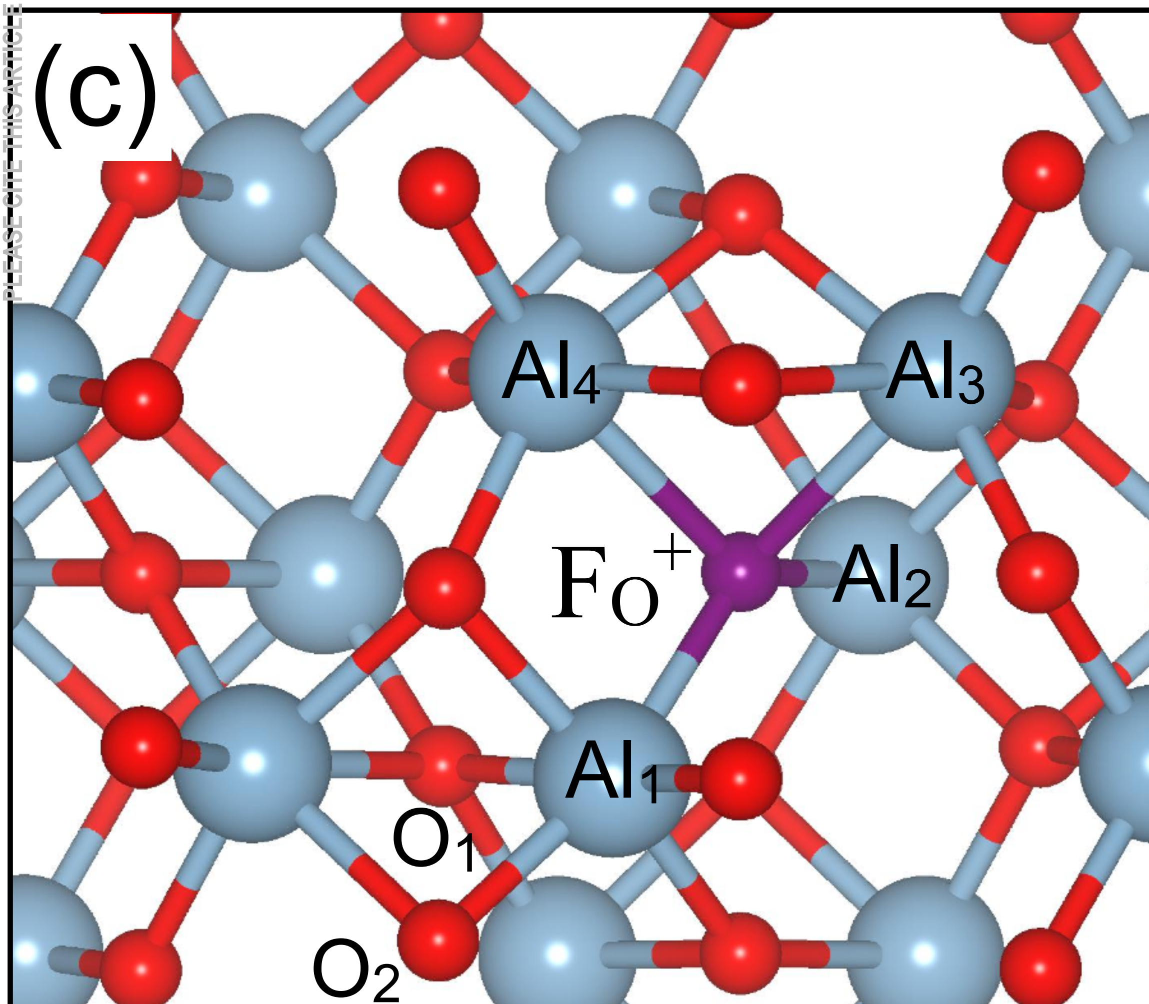

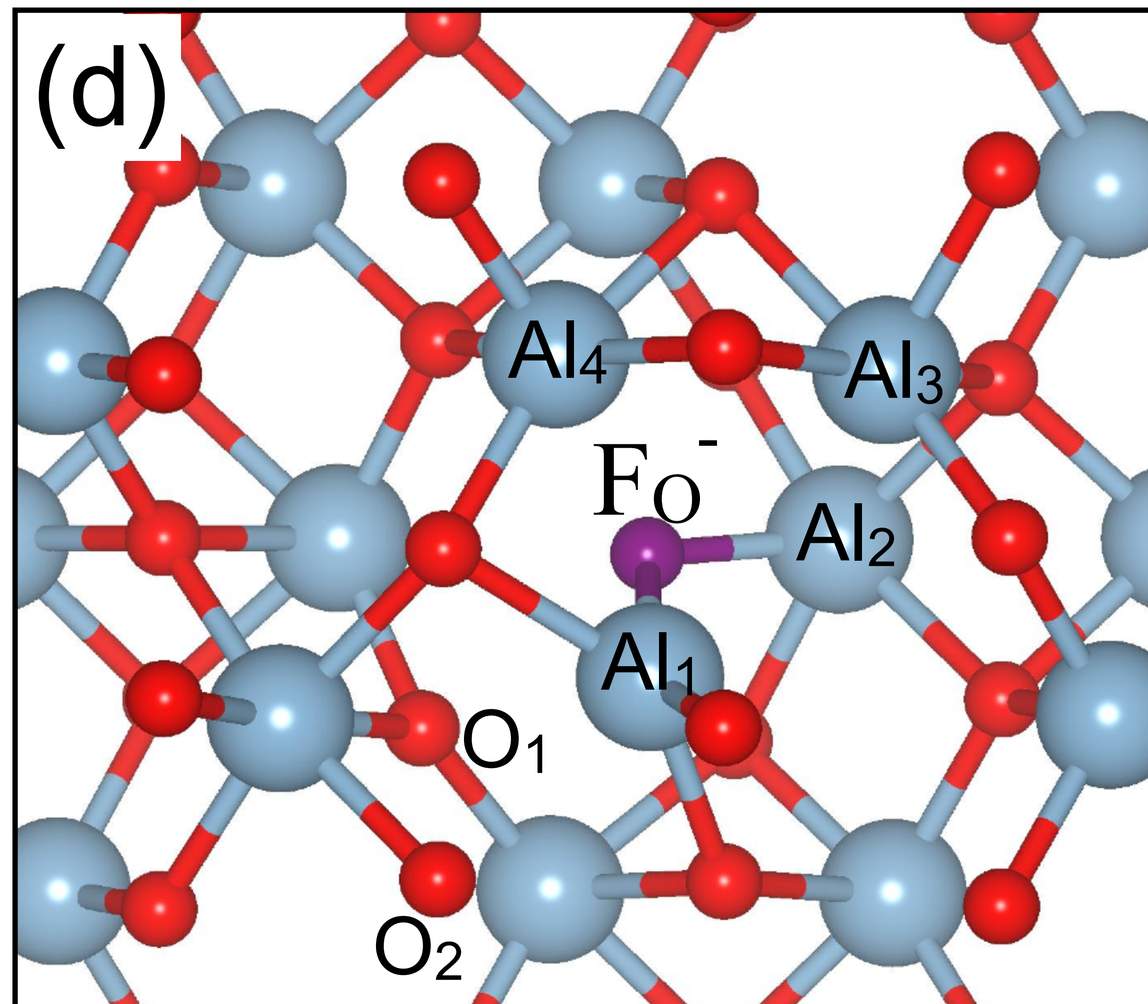

ACCEPTED MANUSCRIPT
Journal of Applied Physics
AIP Publishing
This is the author's peer reviewed, accepted manuscript. However, the online version of record will be different from this version once it has been copyedited and typeset.
PLEASE CITE THIS ARTICLE AS DOI: 10.1063/5.0161929

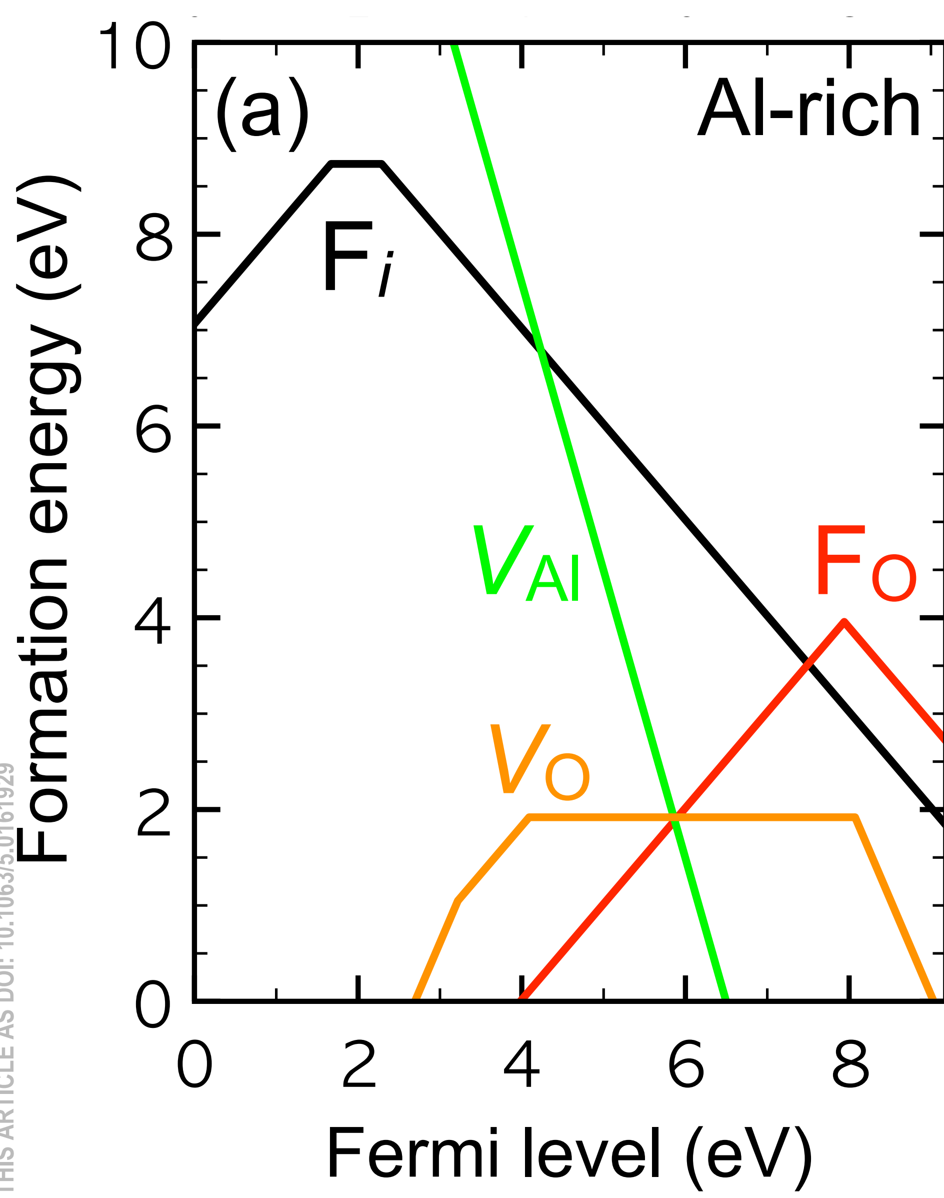

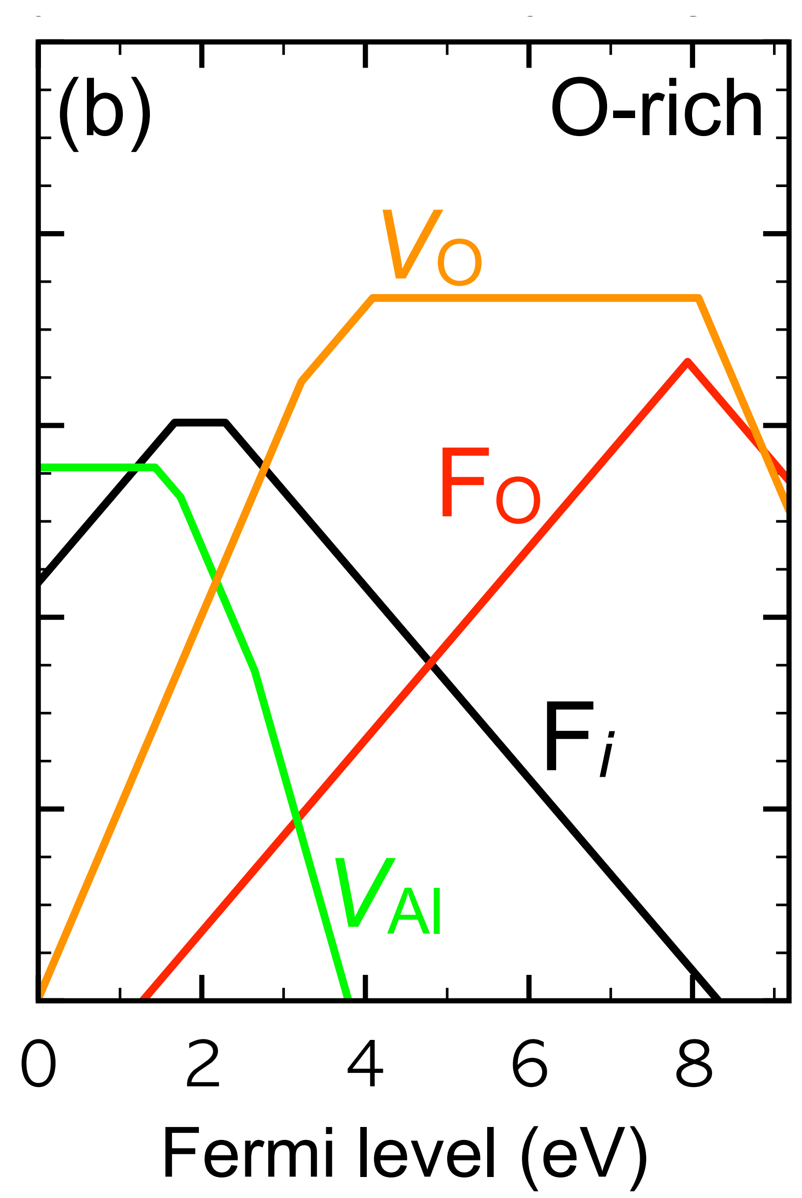

ACCEPTED MANUSCRIPT
Journal of Applied Physics
AIP Publishing
This is the author's peer reviewed, accepted manuscript. However, the online version of record will be different from this version once it has been copyedited and typeset.
PLEASE CITE THIS ARTICLE AS DOI: 10.1063/5.0

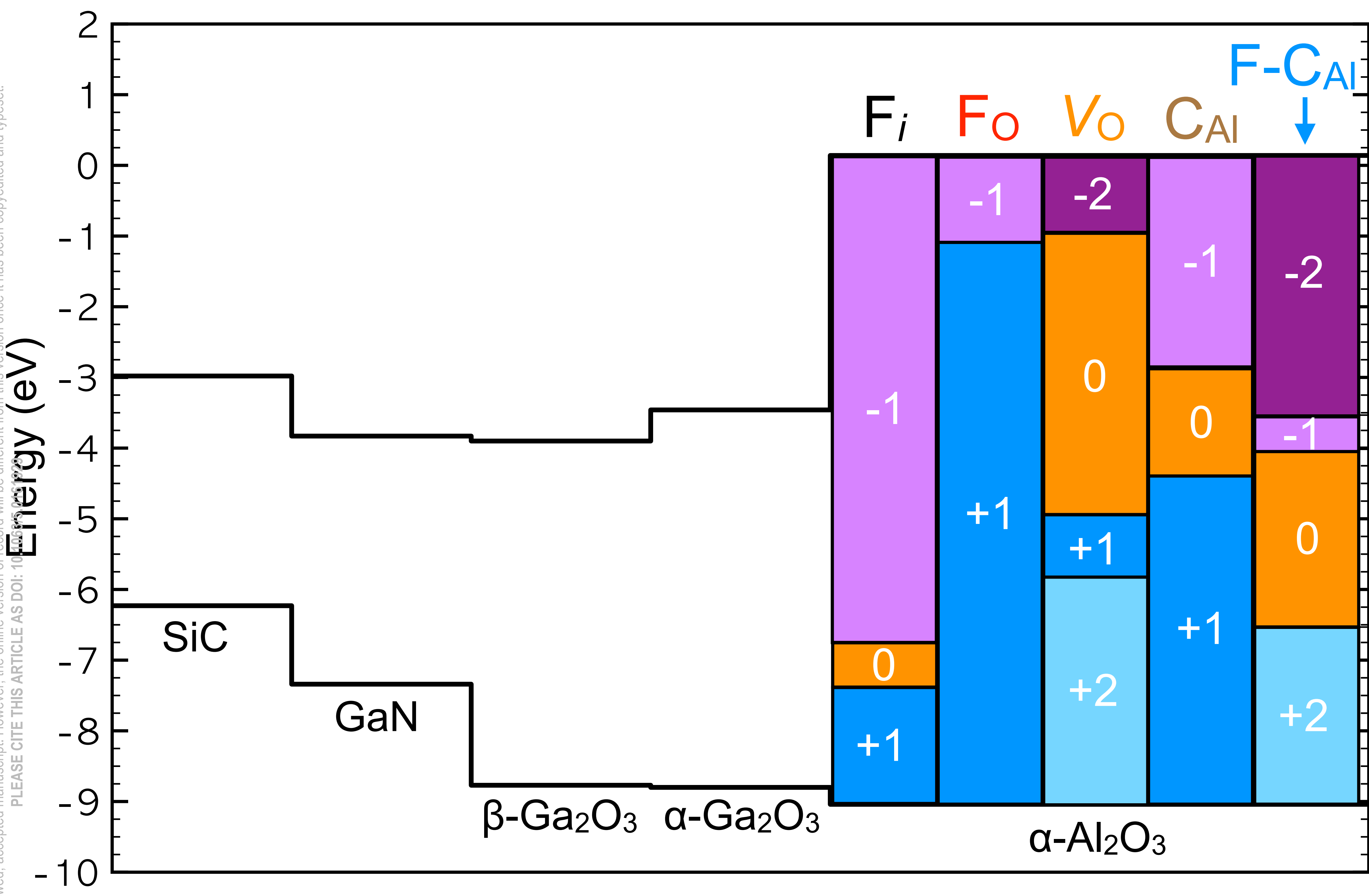

ACCEPTED MANUSCRIPT
Journal of Applied Physics
AIP Publishing
This is the author's peer reviewed, accepted manuscript. However, the online version of record will be different from this version once it has been copyedited and typeset.
PLEASE CITE THIS ARTICLE AS DOI:

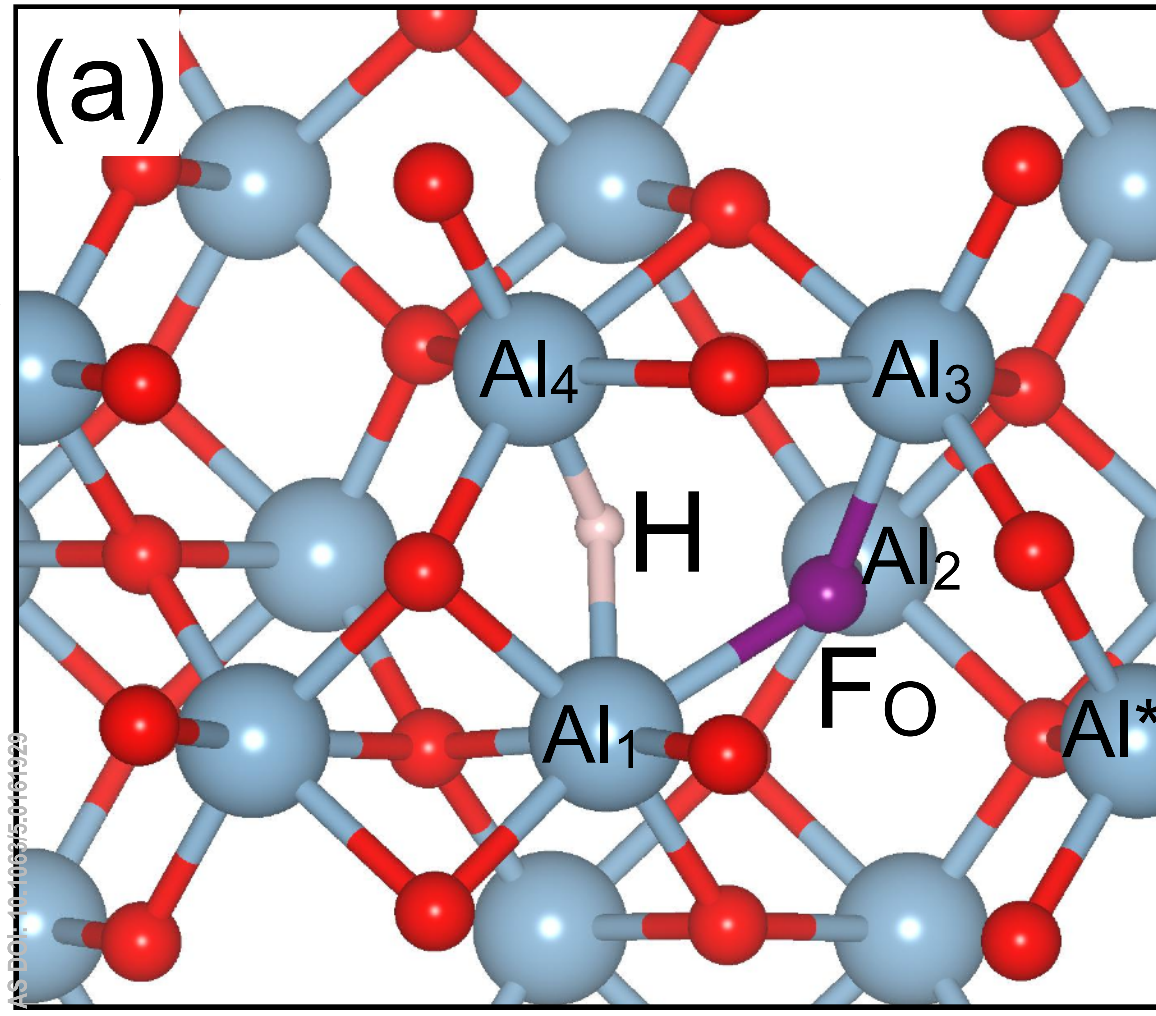

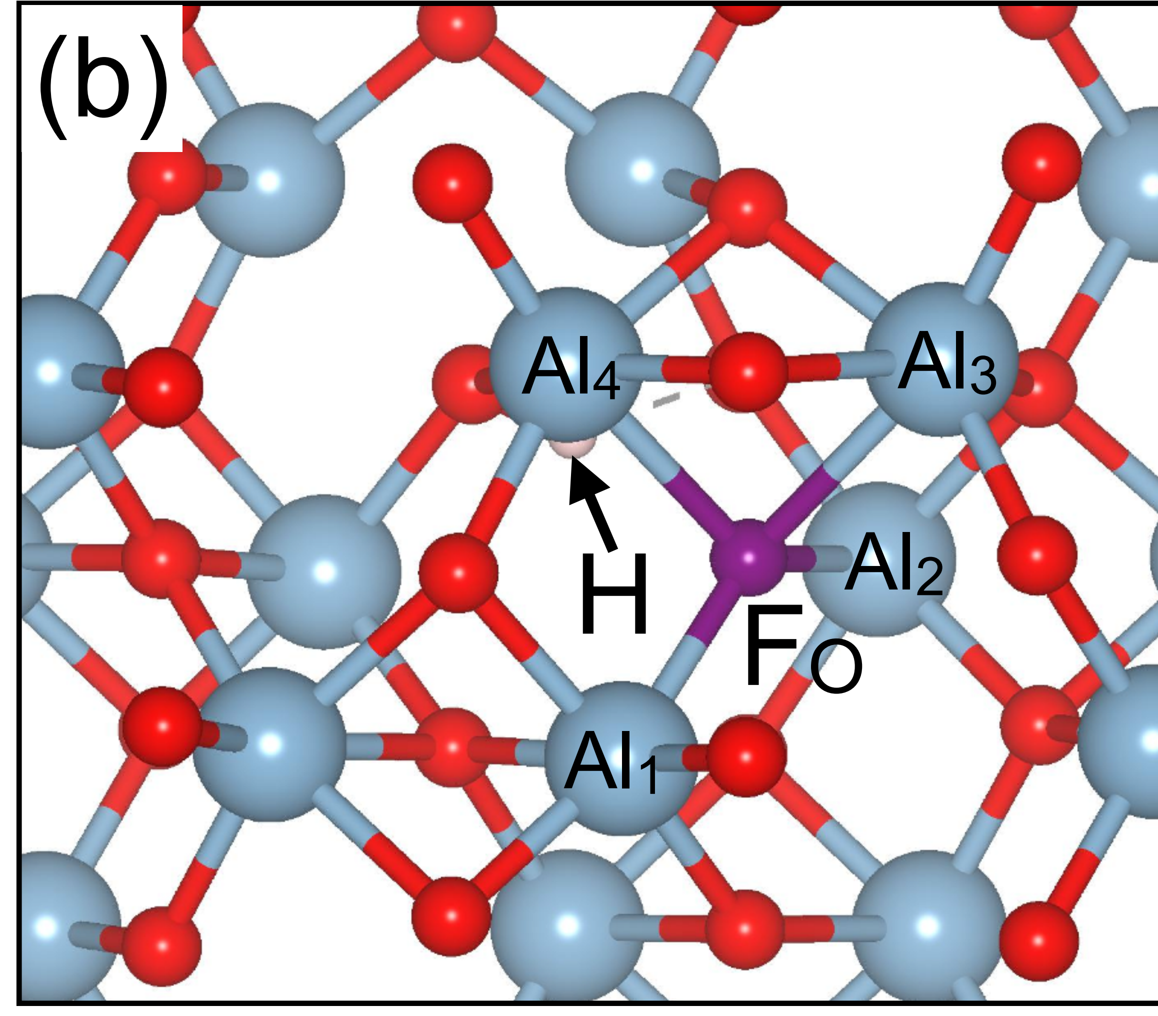

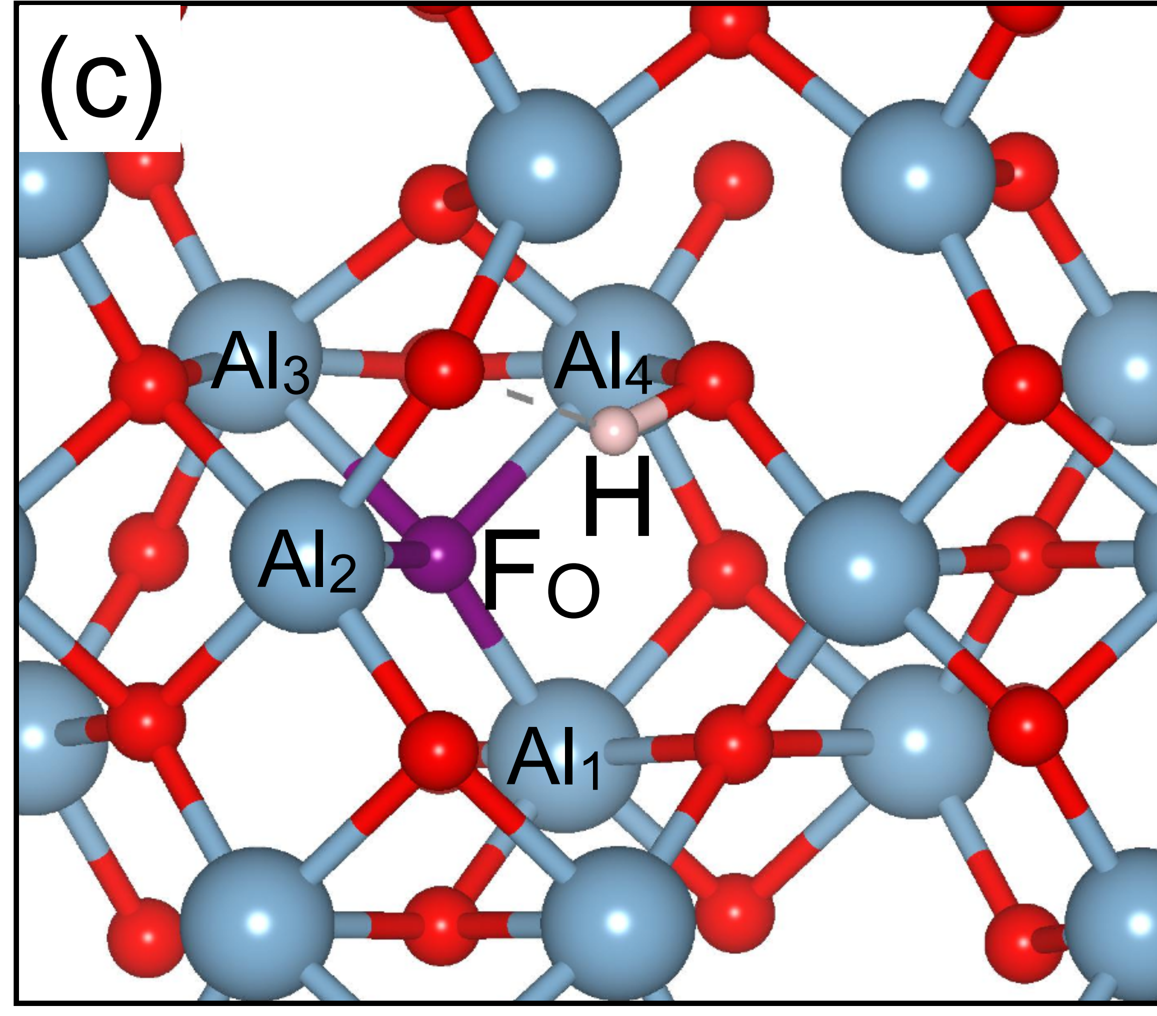

ACCEPTED MANUSCRIPT
Journal of Applied Physics
AIP Publishing
This is the author's peer reviewed, accepted manuscript. However, the online version of record will be different from this version once it has been copyedited and typeset.
PLEASE CITE THIS ARTICLE AS DOI: 10.1063/5.0161929

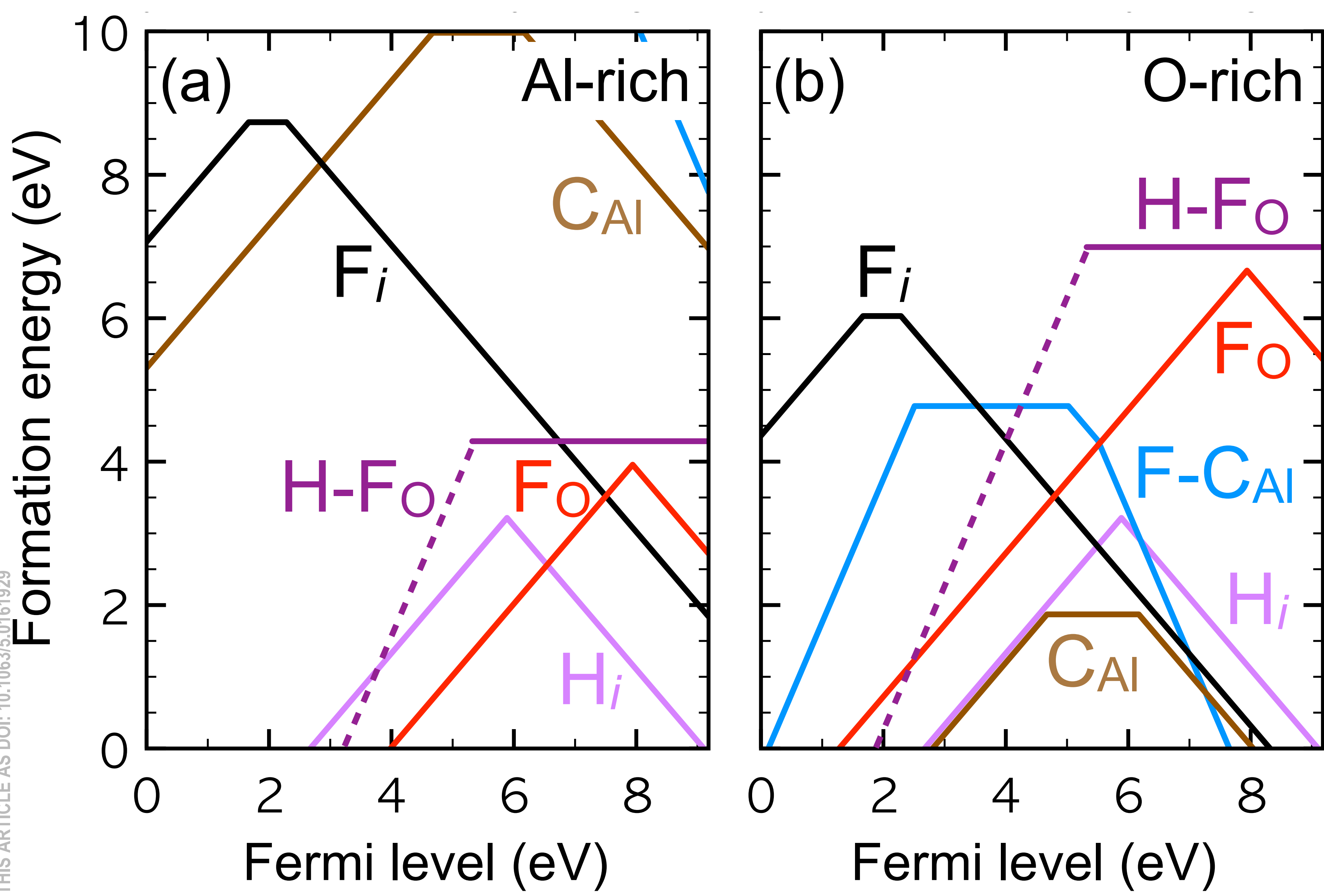

ACCEPTED MANUSCRIPT
Journal of Applied Physics
AIP Publishing
This is the author's peer reviewed, accepted manuscript. However, the online version of record will be different from this version once it has been copyedited and typeset.
PLEASE CITE THIS ARTICLE AS DOI: 10.1063/5.0161125